Interplay between Lipid Interaction and Homo-coiling of Membrane-Tethered Coiled-Coil Peptides

Martin Rabe,[*,†] Harshal R. Zope,[‡] and Alexander Kros[*]

Leiden Institute of Chemistry—Supramolecular and Biomaterial Chemistry, Leiden University, Einsteinweg 55, 2333CC Leiden, The Netherlands

S *Supporting Information*

ABSTRACT: The designed coiled-coil-forming peptides E [(EIAALEK)$_3$] and K [(KIAALKE)$_3$] are known to trigger efficient membrane fusion when they are tethered to lipid vesicles in the form of lipopeptides. Knowledge of their secondary structure is a key element in understanding their role in membrane fusion. Special conditions can be found at the interface of the membrane, where the peptides are confined in close proximity to other peptide molecules as well as to the lipid interface. Consequently, different structural states were proposed for the peptides when tethered to this interface. Due to the multitude of possible states, determining the structure solely on the basis of circular dichroism (CD) spectra at a single temperature can be misleading. In addition, it has not yet been possible to unambiguously distinguish between the membrane-bound and the coiled-coil states of these peptides by means of infrared (IR) spectroscopy due to their very similar amide I′ bands. Here, the molecular basis of this similarity is investigated by means of site-specific ^{13}C-labeled FTIR spectroscopy. Structural similarities between the membrane-interacting helix of K and the homo-coiled-coil-forming helix of E are shown to cause the similar spectroscopic properties. Furthermore, the peptide structure is investigated using temperature-dependent CD and IR spectroscopy, and it is shown that the different states can be distinguished on the basis of their thermal behavior. It is shown that the two peptides behave fundamentaly differently when tethered to the lipid membrane, which implies that their role during membrane fusion is different and the mechanism of this process is asymmetric.
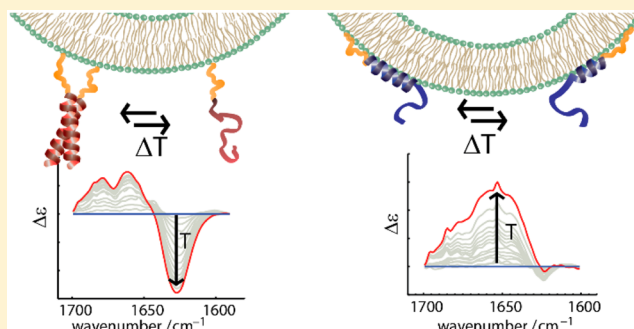
INTRODUCTION

The hallmark of biological membrane fusion is the specific content mixing between two separate enclosed compartments without leakage. This makes this process an interesting target for supramolecular and biomaterials chemists as it opens a route to applications in biotechnology and drug delivery. Consequently, model systems have been designed with the aim of enabling membrane fusion by means of simple, synthetic molecules.[1−3] Among those, membrane-tethered coiled-coil-forming lipopeptides whose design has been inspired by natural SNARE (soluble NSF attachment protein receptor) proteins have been examined extensively in different studies because they were shown to trigger specific and leakage free full fusion of vesicles.[1,4−15] The lipopeptides used here consist of a cholesterol lipid anchor connected via a polyethylene glycol (PEG$_{12}$) spacer to the peptide moieties (lipopeptides CPE, CPK; Chart 1A). The peptide recognition unit is made of two hetero-coiled-coil-forming peptides called E [(EIAALEK)$_3$-NH$_2$] and K [(KIAALKE)$_3$-NH$_2$]. Coiled-coils are peptide complexes consisting of several α-helices that wind around each other. In their primary structure they show a specific arrangement of hydrophobic (h) and polar (p) amino acids in the so-called heptad repeat: *hpphppp*. The positions in this pattern are denoted *abcdefg* (Chart 1B).[16]

If two batches of vesicles bearing CPE and CPK on their membrane are mixed, these vesicles show full fusion.[4,5,8] Although this capability has been extensively studied and the improvement of this system by means of synthetic variation of its components is an ongoing process, the detailed fusion mechanism and its common features with biological membrane fusion remain unclear. However, this knowledge is crucial for the rational improvement of these systems toward a targeted membrane fusion between artificial and biological membranes.[10]

The initial docking step in this fusion process is triggered by the specific molecular recognition of the two hetero-coiled-coil-forming peptides E and K. The docking brings the two membranes into a close proximity. The peptide pair was designed rationally to form specific E/K heterodimers.[17] However, the membrane-tethered peptides can also have other interactions that were not intended in the initial lipopeptide design. Recent experimental and molecular dynamics (MD) studies showed that K interacts with lipid membranes, incorporating as an amphipathic α helix parallel to

Chart 1. (A) Chemical Structures of CPK and CPE Lipopeptides Used in This Study, and Helical Wheel Projections[16] of (B) E/K Coiled-Coil Complex and (C) Monomeric α Helices of K and E, Respectively[a]

gabcdef
CPK: R= -(KIAALKE)$_3$-NH$_2$
CPE: R= -(EIAALEK)$_3$-NH$_2$
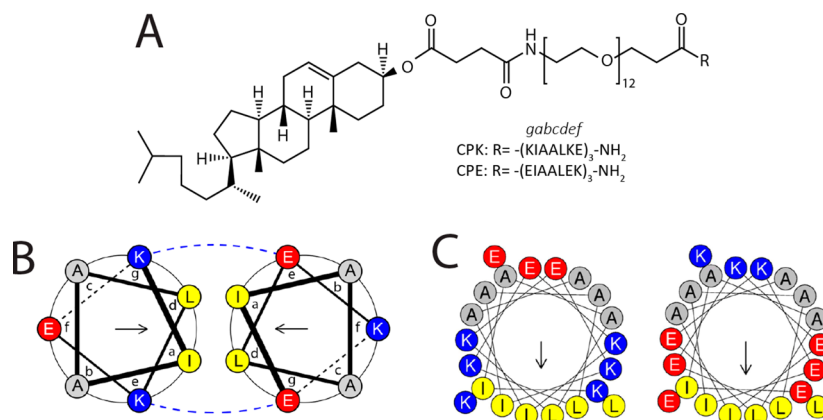
[a]Arrows indicate the direction of the hydrophobic moment.

the lipid interface.[15,18,19] This interaction is anticipated to be a necessary requirement for subsequent steps in the fusion process as it provides the obligatory distortion of the membranes that enable full merging.[15,20] Furthermore, both E and K tend to form homodimers in aqueous buffer.[21] Both peptides have low folding constants for the homodimer formation relative to the heterodimer formation, but at high local concentrations, as found on the surface of vesicles, the peptides might tend to form homomeric aggregates. This means that, prior to the docking step, the membrane-tethered E and K can be in equilibrium between an unordered unbound state and different helical states: homo-coiled or membrane-bound.

In recent fusion studies, circular dichroism (CD) spectroscopy has been used to estimate the helical content of the peptides, because it is a quick and widely used technique that allows the direct study of vesicle-tethered lipopeptides as used in the fusion experiments. Generally, the vesicle-tethered lipopeptides exhibit increased helical contents compared to their untethered equivalents E and K. This was always attributed to the formation of homo-coils E/E and K/K, and peptide membrane interactions were not taken into account.[1,4−10] Typical CD spectra of α-helices exhibit two minima around 208 and 222 nm. Due to the low absolute ellipticity of other secondary structure elements at this position, the mean residual ellipticity at 222 nm ($[\theta]_{222\,nm}$) is a convenient measure for helical content.[22,23] However, by using $[\theta]_{222\,nm}$ only, it is not possible to distinguish whether the origin of this helicity is due to homomeric coiled-coil formation or the presence of single α helices. A second criterion which is commonly used for the characterization of coiled-coil complexes by CD is the ratio $[\theta]_{222\,nm}/[\theta]_{208\,nm}$.[17,24] However, $[\theta]_{208\,nm}$ is often perturbed in experiments with vesicles, due to light scattering in this wavelength region. Also, the ratio $[\theta]_{222\,nm}/[\theta]_{208\,nm}$ might lead to inconclusive results in systems with coexisting unordered peptide chains. Therefore, CD data can be ambiguous in the case of complex systems and further analytical methods are required to obtain detailed information.

A potential way to obtain more information from CD data is to monitor thermally induced peptide unfolding. The melting curves can be analyzed to obtain information regarding the molecularity of peptide unfolding processes,[21] and therefore

pose a promising approach to distinguish coiled-coil formation from peptide membrane interaction.

An additional convenient method for the study of peptide and protein structures is Fourier transform infrared (FTIR) spectroscopy. The position of the amide I band, which mainly originates from the carbonyl stretching vibration of the peptide bond is known to strongly depend on its secondary structure.[25] In D$_2$O this band is usually referred to as amide I′. Coiled-coils have been shown to exhibit characteristic amide I′ bands with two main components, which are not observed for single helices.[26−30] This pattern is caused by the different accessibility of the amide carbonyls for the solvent molecules. The carbonyls on the hydrophilic face, especially in the b, c, and f positions of the heptad repeat can form additional hydrogen bonds with the solvent and absorb ~20 cm^{-1} lower than the amides on the hydrophobic face.[29,30] Surprisingly, a similar pattern was also found in amide I′ bands of peptide K interacting with model lipid monolayers using infrared reflection absorption spectroscopy (IRRAS).[15] As an interaction of the peptide as a homomeric coiled-coil with the membrane seems unlikely, it was hypothesized that the pattern arises from a different accessibility of the carbonyls to water, caused by the shallow insertion of the single amphipathic α-helix. This hypothesis allowed fitting of the angle dependency of the IRRA spectra, yielding the model of the helix insertion parallel to the membrane interface. Although a coherent bigger picture resulted from this approach, the origin of the two-band pattern in the lipid-bound form of K remains under investigation, due to lack of reports of comparable effects in literature.[31−34] Therefore, further investigations of the IR spectroscopic properties of the membrane incorporated state of K together with an unequivocal band assignment are necessary to substantiate the helix insertion model. The latter can be done by site specific labeling of the amide with ^{13}C, which is a convenient way to gain structural information for peptides at the residue level.[29,35−41]

In the present work we investigate the state of the vesicle-tethered lipopeptides under the conditions commonly used in the fusion studies. We extend the commonly used CD approach by monitoring melting curves of the coiled-coil-forming peptides E, K and their lipid-tethered equivalents CPE and CPK. This allows an unambiguous determination of the peptide state on the membrane. To verify the results of this approach,

temperature-dependent IR spectroscopy is applied. A detailed analysis of these temperature dependencies by means of singular value decomposition (SVD)[42−44] sheds light on the intrinsic temperature dependencies of the amide I′ two-band pattern and reveals structural properties of the peptides. Furthermore, the origin of the low-absorbing amide I′ component is determined by studying ^{13}C-labeled peptide K, which also reveals structural details of the membrane-bound state of K. Both applied techniques prove that, in these fusogenic vesicles, lipopeptides CPE and CPK are in different states, contrary to previous assumptions. The facile approach via CD melting curves will be useful in future studies that vary the lipopeptide structure to enhance the fusogenity of the lipopeptides.

■ RESULTS AND DISCUSSION

CD of Free Peptides and Vesicle-Tethered Lipopeptides. Melting curves of peptides, monitored by CD spectroscopy, have been shown to contain relevant information about the molecularity of the peptide unfolding.[21] The CD unfolding curves of untethered peptides E and K in the absence and presence of vesicles and tethered to the vesicle interface were measured (Figure 1). In these and all further experiments the
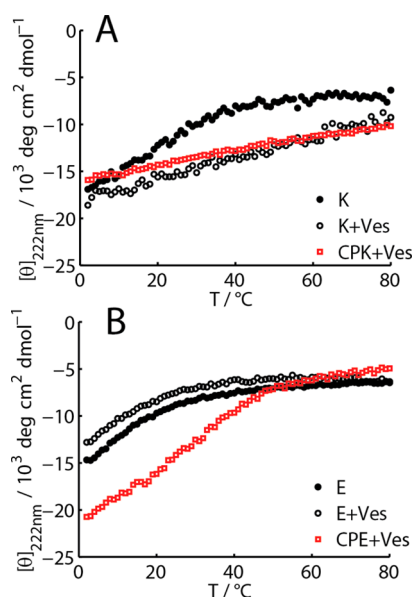

Figure 1. Temperature dependency of ellipticity at 222 nm for (A) K in buffer, K mixed with vesicles, and CPK tethered to vesicles, and for (B) E in buffer, E mixed with vesicles, and CPE tethered to vesicles. Experimental conditions: total peptide concentrations [E] = [K] = 40 μM; [CPE] = [CPK] = 20 μM; [lipid]:[peptide] = [lipid]:[lipopeptide] = 50:1. All measurements in PBS.

lipid composition was DOPC:DOPE:cholesterol (2:1:1), and the buffer was phosphate-buffered saline (PBS, pH 7.4) as used in typical vesicle fusion experiments.[1,4−10] Both free peptides exhibit shifts of the melting curves and the apparent melting temperature T_m toward higher temperatures with increasing peptide concentration (Supporting Information, Figure S1).[21] In general, the T_m of a monomeric peptide chain is independent of concentration, while it is concentration dependent for olgomeric peptide complexes.[45,46] Thus, the observed process is the unfolding of homomeric coiled-coils.

In a mixture with vesicles the $[\theta]_{222\,nm}$ of K was significantly lower over the complete temperature regime; i.e., the helical content was increased (Figure 1A). This is caused by the interaction of the peptide with the lipid bilayer which is accompanied by its folding into an amphipathic helix. Compared to the experiment without vesicles, the shape of the curve appears almost linear with a shallower, uniform slope. In peptide folding studies, similar linear increases of folded coiled-coils are often considered as an intrinsic temperature induced change of the optical properties of the helix that does not relate to significant structural change.[47] Another possibility is that it is caused by non-cooperative changes such as end fraying of helices.[48] In contrast, E in a mixture with vesicles shows a very similar $[\theta]_{222\,nm}$ curve to the lipid free solution (Figure 1B). The slight shift to higher values appears to be caused by light scattering by the vesicles. Thus, the untethered E shows no interactions with the vesicles that induce the formation of a helix.

The different membrane affinities of E and K probably arises from their different charge distribution (Chart 1C).[15] This hypothesis is further enforced by recent MD simulations, where similar membrane affinity differences between E and K were observed.[18,19] In principal both E and K would be able to form a monomeric amphipathic helix that enables them to interact with membrane interfaces. The main difference between the peptides lies in the distribution of the charged amino acids. In the helical wheel projection of K the positively charged lysine residues are distributed perpendicular to the hydrophobic moment, which is a so-called amphipathic α helix of class A according to the classification of Segrest et al.[49] Peptides of this structure are commonly found in apolipoproteins and well known to interact with lipid membranes. For E the distribution is the opposite, a structure which has not been reported to interact strongly with membranes. For the amphipathic A helix it is thought that the relatively long lysine residues can "snorkel", i.e., bend toward the charged lipid headgroup region. This increases the hydrophobic face of the peptide, leads to a higher penetration depth of the peptide and hence to a stronger lipid binding.[18,49−51]

The membrane-tethered CPK also shows decreased $[\theta]_{222\,nm}$ over the measured temperature range. It closely resembles K mixed with vesicles, indicating similarities in the structures and binding states of the peptides (Figure 1A). Based on $[\theta]_{222\,nm}$ at 25 °C, the helicity was found to be 45% and 48% for K and CPK, respectively. Assuming that all peptides are membrane bound, this would imply that the peptides are only partially folded as a helix. However, from this data one cannot determine whether the observed helicity originates from a single state, populated by all peptide molecules or multiple states, differently populated.

CPE, in contrast, shows a $[\theta]_{222\,nm}$ curve that differs from its untethered equivalents (Figure 1B). A lower ellipticity was found, that increases up to ∼50 °C where the curve approaches those of the untethered peptides. This increase in helical content is generally attributed to the homo-coiling of the peptides.[1,4−10] To scrutinize this, further experiments were performed by varying the lipopeptide concentration in the vesicles (Figure S3). CPK showed no significant changes in the temperature-dependent $[\theta]_{222\,nm}$ with concentration change. In contrast, the $[\theta]_{222\,nm}$ curves of CPE shifted slightly to lower temperatures with decreasing concentration. The derivatives do not consist of a single peak, indicating that the observed transition is not a simple two state unfolding. Consequently,

fitting the data with several cooperative melting models with molecularities in the range $n = 2, ..., 5$ yielded insufficient results (data not shown). The maxima in the first derivative also illustrate the shift of the apparent melting temperature T_m (Figure S3B, inset). Therefore, it shows that the unfolding of the peptide on the membrane is of a molecularity bigger than 1, meaning it is a coiled-coil complex.[21,45,46]

The folded fraction (α) of peptide can be determined from the ellipticities at fully folded (θ_F) and fully unfolded (θ_U) states. Assuming values for a coiled-coil with high helical content,[23] of $\theta_F = -32\,000$ deg cm^2 dmol^{-1}, and $\theta_U = -5000$ deg cm^2 dmol^{-1} the value of $[\theta]_{222\,nm}$ at 25 °C of 1 mol% CPE one can estimate that more than 37% of the CPE molecules are folded as homo-coils in a standard vesicle fusion experiment.

The melting of the untethered E and K showed that they are able to form homo-coils at relatively low folding constants, K_F, compared to the E/K hetero-coil (Supporting Information, Table S1). However, when tethered to the interface of the vesicles the local peptide concentration is drastically increased. This leads to a dramatically increased T_m of CPE compared to the untethered E, despite the fact that the overall concentration is lower (Figure 1B). Using the experimental conditions of the melting curves in Figure 1B, this effect can be illustrated: the mean molecular density in a 40 μM solution of untethered E is ~24 000 molecules/μm^3, which is slightly less than the number of peptides that are confined to the lipid bilayer interface (~33 000 molecules/μm^2) at 2% lipopeptide concentration and an average area of 60 Å^2 per lipid. It is clear that this corresponds to an immense agglomeration of molecules and thus to a high local concentration. This explains the substantial amount of homo coiling of CPE on the vesicles.

Similar experiments using vesicles with both lipopeptides present in the same sample did not yield reliable results, as membrane fusion occurred in these samples, which led to strong light scattering and sedimentation during CD and IR measurements (data not shown).

IR Spectroscopy of Peptides in Solutions. FTIR spectroscopy is a common technique to determine the secondary structure of peptides and proteins, because the position of the amide I′ band is strongly influenced by its secondary structure and hydrogen bond formation. Also, the melting processes that were followed by CD spectroscopy are expected to manifest in this band.[40,44,52]

First, the IR spectra of E, K, and E/K in PBS prepared from D$_2$O (d-PBS) were measured at 5 °C. At a total peptide concentration of 1 mM these peptides are expected to predominantly exist in the coiled-coil state at low temperatures. Accordingly, the amide I′ bands of the peptides are all dominated by two main components at ~1630 and ~1649 cm^{-1}, which is a typical pattern for coiled-coils (Figure 2A). The origin of the additional small component at 1668 cm^{-1} is not clear but might be caused by residual trifluoroacetic acid (TFA) from the peptide purification, which is commonly found in this region.[53] Additionally, at 1564 cm^{-1}, the carbonyl stretching mode of the glutamic acid side chains can be found.[54]

The positions of the underlying components in the amide I′ band were determined from the maxima in the smoothed second derivative. With this the shape of the bands could be adequately fitted with three Gaussians in these positions (Figure 2A, Table S2). The results of the band fitting procedures are detailed in the Supporting Information (Tables S2 and S3). Unless otherwise stated, all band fitting procedures
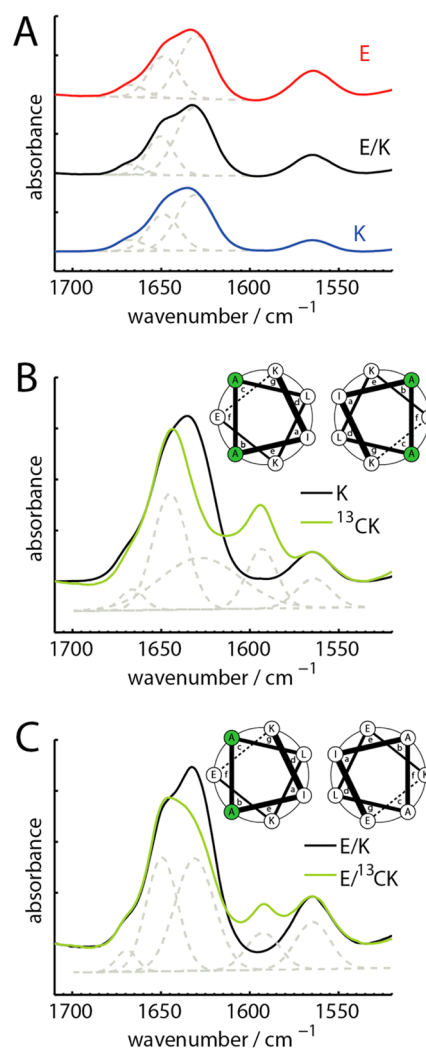

Figure 2. FTIR spectra (solid lines) and fits of the amide I′ bands with gaussians (broken lines) of (A) E, E/K, and K ([peptide] = 1 mM); (B) K and ^{13}CK, and (C) E/K and E/^{13}CK. (B,C) Only fitted amide I′ bands of ^{13}C-labeled peptides are shown which are offset for clarity (broken lines). Spectra were normalized with respect to the C═O stretching band of glutamic acid at 1565 cm^{-1}. Insets show helical wheel projections of dimeric coiled-coils with the position of the ^{13}C-labeled alanine residues highlighted in green. Experimental conditions for all spectra (A)−(C): $T = 5$ °C, [peptide] = 1 mM, in d-PBS.

yielded well separated peaks according to the 95% confidence intervals. The relative absorbance ratios of the two main components at 1630 and 1649 cm^{-1} (A_1/A_2) was determined. The lower A_1/A_2 ratio of E (1.75) and K (1.82) compared to E/K (2.45) might arise from contributions of unordered structures. These are expected to overlap as a broad band centered at ~1645 cm^{-1} (see below) and cannot be resolved in this manner. The addition of more than three bands will also result in an adequate description of the band shape and underlying hidden contributions cannot be excluded. For instance, Pähler et al. used five strongly overlapping bands to describe the amide I′ band of an E/K variant tethered to a supported lipid bilayer.[14] However, these bands appear overfitted and the authors state no rationale for this model. Since the simpler pattern with two main bands reported here can be explained with a consistent physical model, this interpretation is used.

The two main components of the amide I′ band originate from the heterogeneous environment of the helix in the coiled coil.[26−30,33,55] The frequency of the amide I′ band is known to shift down by ~20 cm^{-1} per hydrogen bond to the amide carbonyl. The carbonyls on the hydrophobic face of the coiled-coil exclusively form intramolecular hydrogen bonds in the common i to i+4 manner. On the other side, carbonyls on the hydrophilic face are available for one additional hydrogen bond from the solvent, which lowers their frequency.

To test this model, a variant of K was synthesized with the alanine residues situated in the b and c positions of the heptad repeat containing ^{13}C-labeled carbonyls (^{13}CK). The isotope effect is known to specifically lower the amide I′ position of the labeled residue by 35−40 cm^{-1}.[29,35−41] The IR spectra of ^{13}CK and E/^{13}CK at 5 °C showed strongly reduced intensities at 1630 cm^{-1} compared to their unlabeled equivalents (Figure 2B,C). Additionally a band at ~1592 cm^{-1} arose, the amide I′ band of the ^{13}C-labeled carbonyls. The amide I′ bands of ^{13}CK and E/^{13}CK could be fitted with 4 Gaussian bands. The carbonyl band of glutamic acid was included in the fit at 1564 cm^{-1}, to enhance the band shape modeling at low frequencies. The fit of E/^{13}CK yielded A_1/A_2 = 1.24, which is smaller than the value for E/K of 2.45 showing that the absorbance at 1630 cm^{-1} is significantly reduced (Table S2, Figure 2C). It is expected that some absorbance remains at 1630 cm^{-1} because the amide I′ bands of the amino acids in the f position is expected at this wavenumber.[29] The amide I′ band of the e and g positions have not been studied in detail yet. However, for ^{13}CK, no specific, narrow band for the remaining ^{12}C carbonyls on the hydrophilic face at ~1630 cm^{-1} could be resolved. Instead, band fitting yielded a relatively broad band at ~1628 cm^{-1}, which might be the result of an overlap of the expected hydrogen-bound ^{12}C carbonyl and contributions from coexisting random structures. Nevertheless the reduction of the water-exposed helix band in this position is obvious (Figure 2B).

The reduced absorbance shows that the 1630 cm^{-1} component consists mainly of contributions from the alanine residues, which are situated on the hydrophilic face of the amphipathic helix in the b and c positions of the heptad repeat. This is further strengthened by the position of the ^{13}C amide I′ at ~1592 cm^{-1} corresponding to an isotope shift of ~38 cm^{-1}, which is in range of the typical values of 35−40 cm^{-1} reported for different model peptides independent of their secondary structure and hydrogen-bonding state.[29,35−41] Manas et al. reported the position of ^{13}C-Ala in the b and f positions of a GCN4-p1′ leucine zipper with 1587 cm^{-1} whereas a ^{13}C-Leu in the d position, i.e., the hydrophobic face of the same peptide absorbed at 1607 cm^{-1}.[29] Thus, the position found in the present study reflects the expectation for a water-accessible helical ^{13}C amide I′ band.

IR of Lipopeptides. Next, the spectra of the lipopeptides CPE and CPK tethered to lipid vesicles were measured (Figure 3A). Just as for untethered E and K, the amide I′ bands were dominated by two main components. Taking into consideration the strong absorbance of the lipid C=O stretching band at ~1740 cm^{-1}, the amide I′ bands were fitted with Gaussians yielding A_1/A_2 values of 1.52 and 1.03 for CPE and CPK, respectively (Table S3). For CPE this result is in line with the assumption that the peptide forms homo-coils on the vesicle interface. For CPK, this band shape is similar to amide I′ bands found in IRRA spectra from lipid monolayers containing the lipopeptide LPK with a DOPE anchor.[15] Although the peptide moieties in these molecules are thought to interact as
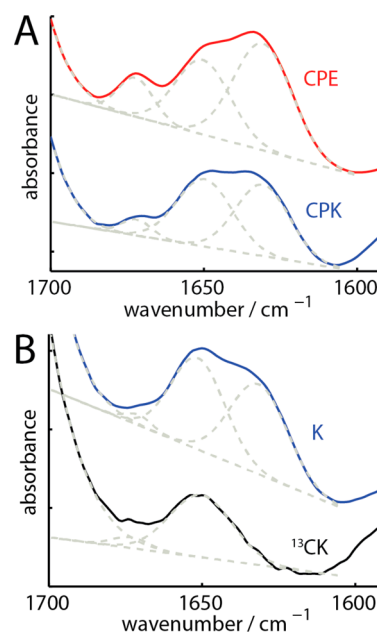

Figure 3. FTIR spectra (continuous lines) of vesicle-tethered (A) CPE and CPK; (B) K at 5 °C and ^{13}CK at 10 °C mixed with vesicles at [lipid]:[peptide] = 200:1; [peptide] = 100 μM and fits of the amide I′ bands with Gaussians (broken lines). All measurements in d-PBS.

monomers with the lipid bilayers, they show the typical amide I′ band shape of multimeric coiled-coils. However, K is thought to insert as an amphipathic A helix into one leaflet of the lipid bilayer with its helical axis parallel to the membrane interface.[15,18] This would also result in a shielding of the hydrophobic face from water. The water density in DOPC bilayers is known to drop significantly below the lipid phosphate group.[56] This can explain the appearance of two amide I′ components that can be attributed to solvent-accessible and inaccessible carbonyls.

Although the assignment of water-accessible and buried amide I′ helical bands in coiled-coils is a well-studied phenomenon in solution,[26−30,38,44,55,57,58] the related effect in a lipid membrane is reported only scarcely by other groups. A variable two-band pattern was reported by Bi et al. for an S-palmitoylated N-terminal peptide of pulmonary surfactant peptide SP-C interacting with DPPC monolayers.[31] The authors interpreted a change of the relative band intensities with respect to each other as the expelling of helical fragments of the peptides from the monolayer, leading to a variation in hydration of the helix. Mukerjhee et al. found amide I′ bands with solvent-accessible and buried components for alanine-rich helical peptides, and amphipathic helices in reverse micelles that mimic membrane water interfaces.[33,34]

To verify the assignment of the two main bands to water-exposed and buried helices, the IR spectra of untethered K and ^{13}CK when interacting with vesicles were measured. Due to the need of a relatively high [lipid]:[peptide] ratio (200:1) the peptide concentration is relatively low in these experiments and the spectra are markedly affected by residual H_2O below 1600 cm^{-1} and the strong lipid C=O band above 1700 cm^{-1}. While the influence of the lipid C=O could be modeled by fitting additional large Gaussian bands, contributions below 1600 cm^{-1} could hardly be resolved. Despite that, the distinct two-band pattern described above can be found in the amide I′ band of K in the membrane, with A_1/A_2 being 1.05, similar to CPK
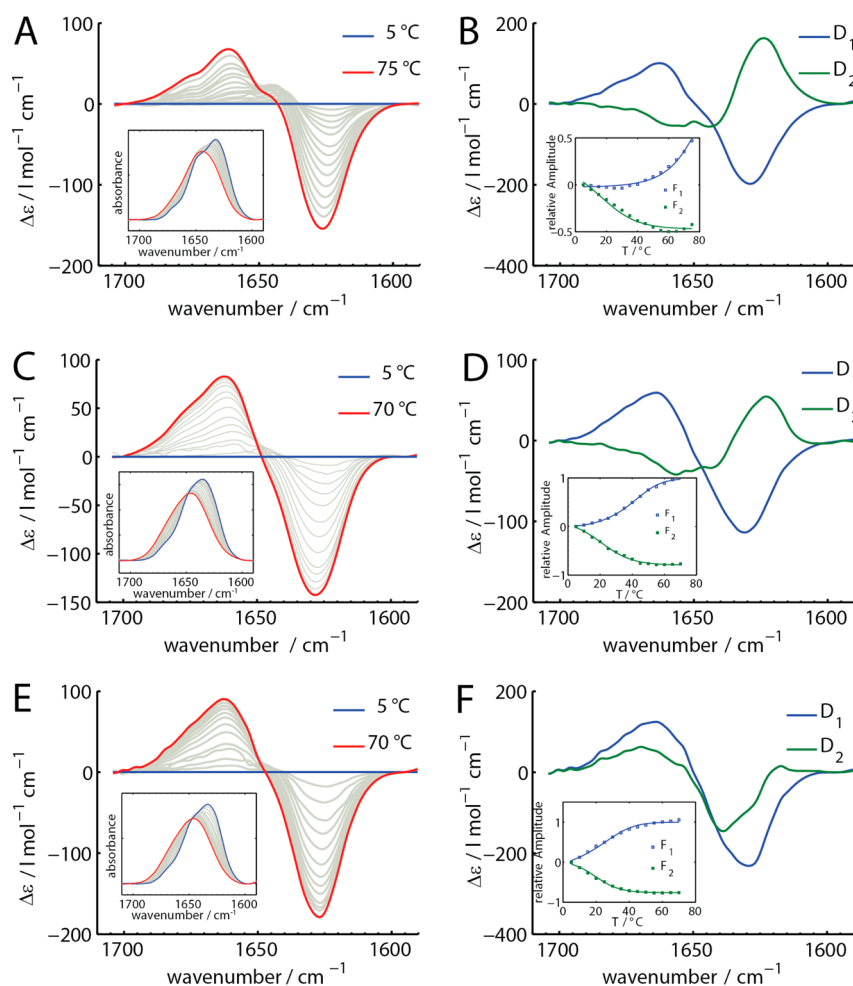
Figure 4. Temperature dependency and singular value decomposition of amide I′ bands for (A,B) E/K, $T = 5-75$ °C; (C,D) K, $T = 5-70$ °C; and (E,F) E, $T = 5-70$ °C. (A,C,E) Temperature-dependent difference spectra in the amide I′ region with amide I′ bands in the insets in 5 °C steps. (B,D,F) Results of singular value decomposition D_1 and D_2 spectral components and F_1, F_2 temperature profiles (squares) and fit results (lines) in the insets; [peptide] = 1 mM, in d-PBS.

(Figure 3B, Table S3). Strikingly, the amide I′ band of ^{13}CK in the membrane showed a strongly reduced absorbance at 1630 cm^{-1} and no contribution at this position was necessary to fit the band shape. Remaining bands in this position could not be resolved due to the relatively low peptide signal. The reduced absorbance at 1630 cm^{-1} implies a high structural similarity of the membrane-bound and the homo-coiled state of K. In both helices the alanine amide carbonyls are accessible for hydrogen bonds from water. A monomeric amphipathic A helix was proposed to be the membrane interacting species of K.[15,18] In this structure the alanine residues are also expected to be situated on the hydrophilic face, which is in common with their ^{12}C amide I′ absorbance at ∼1630 cm^{-1}. The remaining peak, mainly centered at 1650 cm^{-1}, is also in common with remaining absorbance of mostly buried ^{12}C amides of the hydrophobic face.

The relatively low A_1/A_2 ratios of CPK and K interacting with vesicles, compared to CPE or the homo coils of E, K and E/K might be caused by higher amounts of unordered structures (Tables S2 and S3). This correlates well with the helicity values found by CD spectroscopy. However, it is difficult to distinguish if unstructured contributions are caused by unfolded domains within individual chains with all peptides being membrane bound or by the existence of different peptide

populations, i.e., helical and unstructured. Certain arguments speak for the former. An unstructured form would be expected to be in equilibrium with a homomeric coiled coil and would result in concentration-dependent temperature profiles. The absence of this concentration dependence (Figure S3A), might therefore be interpreted as the absence of different populations and supports the model of partially unfolded peptide chains. A partial unfolding is in common with recent results from Pluhackova et al. Using MD simulations the authors found that K loses up to 25% of its helicity when modeled with atomistic resolution in a lipid membrane environment.[18] Also, short peptides tend to fray at their termini,[41] and these ends might reach out of the membrane remaining unfolded. This means the slight positive slope of the temperature-dependent $[\theta]_{222\,nm}$ might indicate an increasing non-cooperative end fraying, leading to a less folded state at higher temperatures.[48]

Temperature Dependencies of Peptides. The temperature-dependent unfolding of coiled-coils as measured by CD spectroscopy is also reflected in the temperature dependency of the amide I′ bands. Deconvolution of the amide I′ bands of the unfolded peptides E and K at 75 °C yielded broad single bands centered at ∼1645 cm^{-1}, with the TFA shoulder around ∼1668 cm^{-1} (data not shown). Thus, the band of the unfolded peptides overlaps strongly with the two helical bands reported
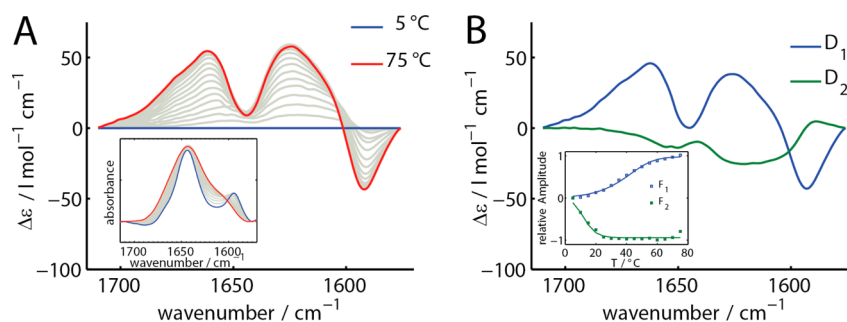
Figure 5. (A) Temperature-dependent difference spectra in the amide I′ region with amide I′ bands in the insets in 5 °C steps of ^{13}CK in d-PBS. (B) Results of singular value decomposition D_1, D_2 spectral components and F_1, F_2 temperature profiles (squares) and fit results (lines) in the insets, $T = 5-75$ °C.
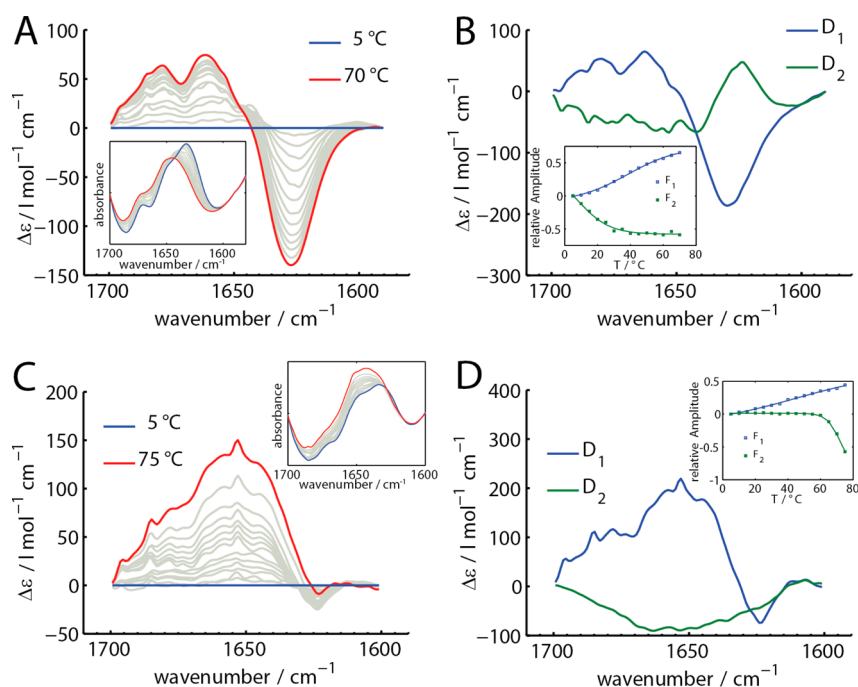

Figure 6. Temperature dependency and singular value decomposition of amide I′ bands for lipopeptides tethered to vesicles in d-PBS: (A,B) CPE, 1 mol%, $T = 5-70$ °C; (C,D) CPK, $T = 5-75$ °C. (A,C) Temperature-dependent difference spectra in the amide I′ region with amide I′ bands in the insets in 5 °C steps. (B,D) Results of singular value decomposition D_1, D_2 spectral components and F_1, F_2 temperature profiles (squares) and fit results (lines).

above. In order to clarify the changes in the amide I′ band upon unfolding, difference spectra of the molar absorptivity per amino acid residue ($\Delta\varepsilon = \varepsilon_T - \varepsilon_{5\,°C}$) are interpreted in the following (Figures 4−Figure 7). These are also sometimes referred to as "fingerprints" of a conformational change because they can be analyzed in terms of their magnitude, shape, and temperature dependence and classified according to their similarity.[54]

The straightforward interpretation of the difference spectra is hampered by the intrinsic temperature dependence of the amide I′ band components and artifacts from residual H_2O in the case of low peptide signals (see below). For instance, the temperature-dependent difference amide I′ bands of E/K clearly show no isosbestic point, which shows that more than one process affects the absorbance band (Figure 4A). The overlapping spectral changes can be separated by means of SVD in combination with a global fitting routine.[42−44] A band can, for example, show an intensity decrease due to a reaction or a structural transition, at the same time this band can shift its

position, due to changes in the strength of hydrogen bonds with temperature. These two spectral components overlap in the resulting difference spectra, both having their own temperature dependency. Under the assumption that the single spectral components have a temperature dependency of a sigmoidal shape, the different components that overlap in the spectrum can be distinguished using SVD. The results of this linear algebraic procedure are the separated spectral components D_1, ..., D_n and their temperature dependencies F_1, ..., F_n (Figure 4B,D,F) which, together, model the original temperature-dependent difference spectra. The resulting D components can be interpreted to reveal molecular details of the temperature-dependent processes. The F components yield the midpoints of the transitions T_{m1}, ..., T_{m2} and their widths and describe the physics of the underlying process more precisely than measuring the absorbance at a single frequency.[44]

For the untethered peptides E, K, and E/K one transition is assumed to be the unfolding of the coiled-coils, which is modeled in the F_1 component with the thermodynamic
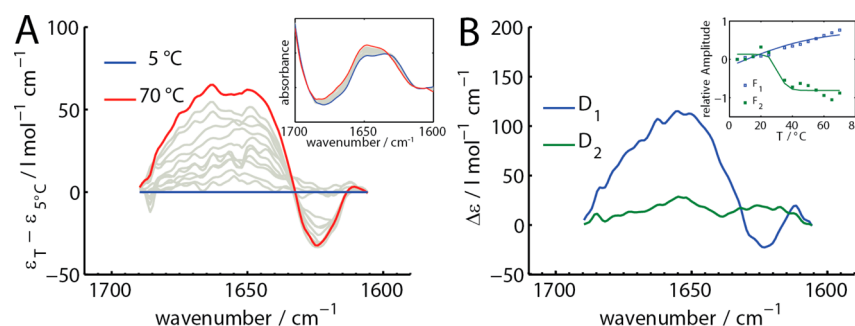
Figure 7. (A) Temperature-dependent difference spectra in the amide I′ region with amide I′ bands in the insets in 5 °C steps of K mixed with vesicles. (B) Results of singular value decomposition D_1, D_2 spectral components and F_1, F_2 temperature profiles (squares) and fit results (lines) in the insets ([K] = 100 μM; [Lipid]:[K] = 200:1, in d-PBS), T = 5−70 °C.

parameters ($\Delta H°$, Δc_P, $T°$) as determined from CD measurements (Table S1). The corresponding D_1 components of all peptides show a striking similarity with a strong and broad negative component centered at ~1630 cm^{-1} and a positive feature at 1660 cm^{-1} (Figure 4B,D,F). The corresponding F_1 thermal components are all ≥0, which means that the unfolding of the coiled-coils is always accompanied by a vanishing of the band at 1630 cm^{-1}. In K and E/K the D_2 components are very similar to a positive feature at ~1624 cm^{-1} and negative intensity in the region 1640−1660 cm^{-1} (Figure 4B,D). Taking into account the negative values of F_2 over the whole temperature regime this corresponds to a blue shift of the water-exposed band of the coiled-coil spectrum. The midpoint of this transition (T_{m2}) is below the melting temperature of the peptides which shows that the process influences the spectra less while the coiled coils melt. This blue shift is a known phenomenon for the water-exposed amide I′ band of coiled-coils. Manas et al. reported that amide I′ bands of water-exposed carbonyls show stronger blue shifts at increasing temperature than buried ones, probably due to the weakening of the additional hydrogen bonds.[29]

The D_2 and F_2 components of E mainly overlap with its D_1 and F_1 components; i.e., in this case the SVD global fitting routine could not resolve additional information (Figure 4F). The low tendency of E to form homo-coils with the lower folding constant K_F at 25 °C (Table S1) leads to the presence of only a small amount of E homo-coils in the measured temperature range. Hence, there is only a small influence of the blue shift of the 1630 cm^{-1} band on the difference spectra.

While the water-accessible amide I′ band vanishes upon melting, the influence of melting on the solvent-buried amide I′ band is found in the difference spectra of ^{13}CK (Figure 5). The D_1 component indicates a broadening of the band at ~1650 cm^{-1}, resulting from the rising of the band of unstructured peptide chains. The negative feature at 1590 cm^{-1} corresponds to the disappearance of the water-exposed ^{13}C amide I′ due to melting and is accordingly observed only in difference spectra ^{13}CK and E/^{13}CK (Figures 5 and S4). The temperature-dependent difference spectra of E/^{13}CK were found to be rather complex due to the multitude of bands. Thus, it is not discussed in detail; however, these spectra did not contradict the results described before (Figure S4).

Taken together the analysis of the temperature-dependent IR difference spectra of E, K, ^{13}CK, and E/K revealed that the thermal unfolding of the coiled-coils can be retrieved by a specific difference spectrum. This "fingerprint" is dominated by a strong absorbance decrease at 1630 cm^{-1} and an increase at 1650 cm^{-1}. This overlaps with a more subtle shift of the water-accessible helical band of the coiled-coil at 1630 cm^{-1} to higher frequencies, which occurs at temperatures below the cooperative melting temperature of the complex.

Strikingly, the thermal difference spectra of membrane-tethered CPE are also dominated by this pattern as can be seen in its D_1 component (Figure 6A,B). The T_{m1} of the corresponding sigmoidal F_1 component is at 38 °C, which lies well in the range of the T_m found in the CD unfolding curves (Figure S3). Furthermore, the D_2 component indicates a slight blue shift of the 1630 cm^{-1} band as was found for the untethered coiled-coils. This data therefore strongly suggest that membrane-tethered E is in a homomeric coiled-coil state, which unfolds upon heating (Figure 8A).

Conversely, the difference spectra of the membrane-tethered CPK and K mixed with vesicles show both D_1 components with a broad absorbance increase at ~1650 cm^{-1} but only a small decrease at 1623 cm^{-1} (Figures 6C,D and 7). These spectral components differ substantially from the D_1 component of CPE and therefore indicate a different transition. The increase at 1650 cm^{-1} was also apparent in the D_1 component of ^{13}CK mixed with vesicles (Figure S5). The decrease at 1623 cm^{-1} appears to arise from the temperature-dependent blue shift of the water-exposed band. It has to be noted that the components found in the D_2 component of these measurements appear to be artifacts arising from variations in the residual H$_2$O concentration in the sample. Band fitting of the spectra at 75 °C revealed that these amide I′ bands still consist of two main components of a similar area at 1635 and 1652 cm^{-1} (Figure S6). Interestingly, the corresponding F_1 components are relatively shallow and almost linear, indicating that the observed D_1 spectral component does not relate to a cooperative transition, which is in line with the almost linear shapes of the $[\theta]_{222\,nm}$ curves of CPK and K mixed with vesicles (Figure 1).

This discussed data show that membrane-bound K exhibits a fundamentally different temperature dependency from an unfolding coiled-coil. Despite the expected blue shift of the water-accessible band, the amide I′ retains its two main components up to 75 °C. Thus, the peptide does not unfold cooperatively and stays bound to the membrane even at temperatures as high as 75 °C (Figure 8B). However, the intermediate helical content, decreasing with temperature found by CD (Figures 1 and S3) and the relatively low absorbance ratio A_1/A_2 (Table S3) indicate a certain contribution of unordered structure in the peptide chains which might, upon heating, increase in a non-cooperative way.
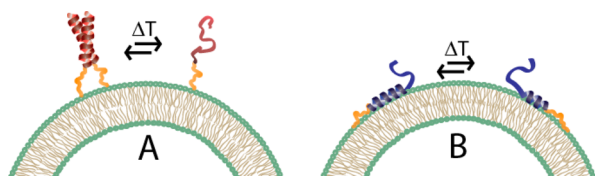
Figure 8. Schematic drawing of temperature-dependent changes of peptide states when tethered to membranes. (A) CPE is predominantly folded in an E/E coiled coil which unfolds and dissociates upon heating. (B) CPK is predominantly bound to the membrane in a helical state and stays bound upon heating.

The prefusion states of the peptides at the membrane, have a direct impact on the fusion mechanism. As soon as CPE and CPK-bearing vesicles are mixed, they dock by formation of the hetero-coiled-coil and membrane fusion starts. The membrane-interacting form of K coexists with the E/K hetero-coiled-coil during and after full fusion.[15] As shown here, this membrane−peptide interaction is of considerable strength, because it is stable up to 75 °C, far above the melting of the K homo-coil. This interaction can deliver the membrane distortion and curvature that is necessary to complete full fusion. K has multiple functions within this mechansim in contrast to its binding partner E, which makes it an asymmetric process. Furthermore, the CD and IR data presented here, show that the coexistence of E homo-coils with the E/K hetero-coils during and after fusion is a further possibility. The prefusion states of both E and K might play a role when fusion goes over several rounds, as reported by Marsden et al.[4] It was stated that the coiled-coil peptides can be employed in repetitive docking-fusion cycles, implying that hetero-coiled-coils are able to dissociate. This is more favorable at the lipid interface than in solution, considering that the prefusion states are the products after dissociation at the membrane.

CONCLUSIONS

The temperature-dependent unfolding of the fusogenic coiled-coil-forming peptides E and K in solution and tethered to lipid vesicles could be followed by CD and difference IR spectroscopy and yielded comparable temperature profiles. Membrane-tethered CPE showed concentration-dependent temperature profiles in CD, typical of an unfolding transition and the IR spectral changes exhibit also the characteristics of coiled-coil unfolding. In contrast, CPK on membranes exhibits no transition, remaining in its membrane-bound state up to 75 °C. The membrane-bound CPK also does not show high helicity, which indicate a partially folded helix in the membrane-bound state.

The IR spectra of membrane-tethered homo-coiled CPE and membrane incorporated, monomeric CPK show remarkable similarities, despite their different states. This is caused by similar accessibilities of the amide carbonyls for water in the coiled-coil and the amphipathic A helix which are both partially hydrophobically buried. These results contribute further to the model of lipopeptide mediated fusion as they show that it is an asymmetric process, meaning that the two complementary units behave fundamentally differently before, during, and after fusion. Furthermore, the results show, that the special conditions at the membrane interface have differing influences on the state of the membrane-tethered peptides, depending on their individual properties. This influence is difficult to predict and has to be studied for each peptide individually for future generations of the lipopeptides.

It was proposed earlier[15] that the interaction of K with the membrane induces curvature which helps to overcome the highly curved intermediate states of lipid reorganization during fusion. Thus, a specific manipulation of the membrane affinity of K appears to be a promising handle to influence the fusion mechanism in future studies. For these future designs, the facile approach demonstrated here, using temperature- and concentration-dependent CD unfolding curves of vesicle-tethered lipopeptides will be helpful in determining the peptide state in the fusion experiments unambiguously.

■ EXPERIMENTAL SECTION

Materials. Fmoc-protected amino acids and Sieber amide resin for peptide synthesis were purchased from Novabiochem, and Fmoc-protected (1-^{13}C, 99%) L-alanine was purchased from Cambridge Isotope Laboratories. DOPC (1,2-dioleoyl-sn-glycero-3-phosphocholine), DOPE (1,2-dioleoyl-sn-glycero-3-phosphoethanolamine), and cholesterol were purchased from Avanti Polar Lipids. Solvents, buffer salts, D_2O, and DCl (deuterium content ≥99.9%) were purchased from Sigma-Aldrich. All water was ultrapure with resistance ≥18 MΩ cm^{-1} and TOC ≤ 2 ppm produced from a Milli-Q Reference A+ purification system. All experiments were carried out in phosphate buffered saline prepared in water (PBS) or D_2O (d-PBS) of the composition 150 mM NaCl, 20 mM PO_4^{3-} at pH/pD 7.4.[59]

Peptide Synthesis. The peptides E [Ac-(EIAALEK)$_3$-NH$_2$], K [Ac-(KIAALKE)$_3$-NH$_2$], and ^{13}CK, with the same sequence as K and a ^{13}C-amide-labeled alanine residue, were synthesized using standard Fmoc-chemistry on a Biotage Syro I and purified by RP-HPLC to yield a purity >95% based on HPLC. Identity of the peptides was determined by LC-MS. The lipopeptides were synthesized and purified as described elsewhere.[5,8] Peptides were solved in 10 mM HCl and lyophilized three times to remove TFA.[53] Peptide stock solutions in d-PBS were prepared at ∼2 mg/mL and diluted accordingly for the measurements. Lipopeptide stock solutions were prepared in a CHCl$_3$:MeOH; 3:1 solution and added to the lipids prior to solvent evaporation.

Vesicle Preparation. Lipid stock solutions of the composition DOPC:DOPE:Cholesterol (2:1:1) were prepared in CHCl$_3$:MeOH 3:1. For experiments with lipopeptides, lipid stock solutions were mixed with CPK and CPE stock solutions to yield mixtures with the desired molar ratio. Lipid films were created by slow evaporation of the solvents under N_2 stream and kept under vacuum overnight. The films were rehydrated with PBS or d-PBS yielding final lipid concentrations of typically 1−2 mM for CD or 20 mM for IR measurements. For measurements with untethered peptides, the lipid films were directly hydrated with solutions of the peptides. Large unilamellar vesicles (LUVs) were formed by sonication at 55 °C for ∼15 min. The size of the vesicles was tested by DLS using a Malvern Zetasizer nano-s and was typically found to be ∼100 nm.

Circular Dichroism Spectroscopy. CD measurements were performed on a Jasco J815 CD spectrometer equipped with a Jasco PTC 123 Peltier temperature controller. Samples were heated in 2 mm quartz cuvettes at a rate of 40 °C h^{-1} in the range 2−95 °C and the elipticity at 222 nm (θ_{222}) was measured as a criterion for α-helicity. CD spectra between 190−260 nm were also collected at T = 5, 25, and 80 °C. Spectra taken at 5 °C before and directly after a full heating cycle were found to be reproducible for all used samples. The mean residual ellipticity [θ] was calculated from the measured ellipticity θ, the path length l, the molar monomer concentration c_M, and the number of amino acids per peptide N by

$$[\theta] = \frac{\theta}{lc_M N} \tag{1}$$

The relative α helicity (rh) was calculated from $[\theta]_{222\,nm}$, the mean residue ellipticity at 222 nm, and N, the number of amino acids per peptide, by[22,23]

$$\text{rh} = \frac{[\theta]_{222\ nm}}{-40 \times 10^3 \text{deg cm}^2 \text{ dmol}^{-1}\left(1 - \frac{4.6}{N}\right)} \times 100\% \tag{2}$$

The fraction of folded peptide α is calculated, using the ellipticity when all molecules are folded or unfolded (θ_F, θ_U), by

$$\alpha = \frac{[\theta] - \theta_U}{\theta_F - \theta_U} \tag{3}$$

Concentration-dependent unfolding curves were used to determine the thermodynamics of folding of the free coiled coil complexes as detailed in the Supporting Information.

Transmission FT-IR Spectroscopy. Transmission FT-IR spectra were measured using a Bio-Rad Excalibur spectrometer equipped with a nitrogen-cooled MCT detector. A temperature-controlled liquid transmission cell with CaF_2 windows and a fixed nominal path length of 50 μm was used. The precise path length (d) was determined by the interference fringe method. Sample spectra in d-PBS and reference spectra of d-PBS at 25 °C were measured at a resolution of 2 cm^{-1}, with a zero-filling factor of 1. Spectra were recorded between 5 and 75 °C in steps of 5 °C. The temperature of the cell was measured and kept constant during measurement at ±0.2 °C. For each spectrum 128 scans were averaged. Several spectra were averaged and corrected by manual subtraction of a water vapor spectrum. The molar absorptivity per residue (ε) was calculated from the absorbance (A), the peptide concentration (c), and the number of amino acid residues per peptide chain (n) according to Beer−Lambert law:

$$\varepsilon = \frac{A}{ncd} \tag{4}$$

For band fitting[60] of the amide I′ the second derivative of the spectra were smoothed for determination of the position of underlying bands. The positions found were used as input for fitting of the band shape with Gaussian peaks on a linear baseline by means of a trust-region-reflective algorithm.

Singular Value Decomposition and Global Fitting. For analysis of difference spectra from baseline corrected molar absorptivity spectra ($\varepsilon_T - \varepsilon_{5\,°C}$) SVD in combination with global curve fitting was applied.[42−44] The data matrix $A(\tilde{\nu},T)$ was created by ordering the difference spectra in such a way that each column corresponds to a temperature. SVD is applied to the data matrix (MatLab function: *svd*) yielding three matrices, U, S, and V^T:

$$A(\tilde{\nu},\ T) = USV^T \tag{5}$$

corresponding to the basis spectra (U), the singular values (S), and the transpose of the temperature development of the basis spectra (V^T). From these matrices components above a rank (r) of 2 were omitted as they mainly contained noise. To describe the data matrix on the basis of overlapping physical transitions, it is assumed that these matrices can be described by a matrix D containing the spectral components of the overlapping components and F^T containing their temperature dependencies:

$$USV^T = DF^T \tag{6}$$

Multiplication with the pseudo-inverse of F^T (F^{T+}) yields

$$D = USH \tag{7}$$

with

$$H = V^T F^{T+} \tag{8}$$

This means the matrix H contains the coefficients determining how the weighted basis spectra (US) must be mixed to yield the spectral component matrix D, and these coefficients can be obtained by globally fitting V^T with physical models for each spectral component. The model used for measurements of lipopeptides or peptides with vesicles consisted of two sigmoid functions:

$$f(T)_n = h_{n1}\left(b_1 + \frac{m_1 - b_1}{1 + \exp\left(\frac{T_{m_1} - T}{\delta_1}\right)}\right)$$
$$+ h_{n2}\left(b_2 + \frac{m_2 - b_2}{1 + \exp\left(\frac{T_{m_2} - T}{\delta_2}\right)}\right) \tag{9}$$

In this equation, subscript n refers to the nth row of the matrix V^T; h_{n1} and h_{n2} are the corresponding elements of H, while b, m, T_m, and δ are the minimum value, maximum value, midpoint, and width of the two sigmoidal transitions. For fitting a trust-region-reflective algorithm (MatLab function: *lsqcurvefit*) was used, leaving the parameters b, m, T_m, and δ global.

For melting of the coiled-coil peptides E, K, and E/K, one transition was assumed to be the thermal peptide unfolding. The parameters $\Delta H°$ and $T°$, the enthalpy and the temperature where the folding constant $K_F = 1$, and ΔC_P, the change in heat capacity upon folding, were determined by CD spectroscopy (see Supporting Information) and set constant during global fitting. In the applied model, the first sigmoid function was replaced by the temperature-dependent fraction of folded peptide $\alpha(T)$:

$$f(T)_n = h_{n1}(\alpha(T)(m_1 - b_1) + b_1)$$
$$+ h_{n2}\left(b_2 + \frac{m_2 - b_2}{1 + \exp\left(\frac{T_{m_2} - T}{\delta_2}\right)}\right) \tag{10}$$

$\alpha(T)$ was calculated using the unfolded fraction β ($\beta = 1 - \alpha$) from the analytical solutions of

$$a\beta^2 + \beta - 1 = 0 \tag{11}$$

as described in detail elsewhere.[21]

The F matrix was determined from

$$F^T = H^{-1}V^T \tag{12}$$

All calculations were performed using MatLab 2013a equipped with curve-fitting toolbox.

■ ASSOCIATED CONTENT

ⓈSupporting Information

The Supporting Information is available free of charge on the ACS Publications website at DOI: 10.1021/acs.langmuir.5b02094.

Determination of peptide unfolding thermodynamics by CD spectroscopy as well as supporting tables and figures (PDF)

■ AUTHOR INFORMATION

Corresponding Authors
*E-mail (M.R.): m.rabe@mpie.de.
*E-mail (A.K.): a.kros@chem.leidenuniv.nl.

Present Addresses
†(M.R.) Department of Interface Chemistry and Surface Engineering, Max-Planck-Institute for Iron Research GmbH, Max-Planck-Str. 1, 40237 Düsseldorf, Germany
‡(H.R.Z.) Laboratory of Nanomedicine and Biomaterials, Department of Anesthesiology, Brigham and Women's Hospital, Harvard Medical School, Boston, MA 02115, USA

Notes

The authors declare no competing financial interest.

■ REFERENCES

(1) Marsden, H. R.; Tomatsu, I.; Kros, A. Model systems for membrane fusion. *Chem. Soc. Rev.* **2011**, *40*, 1572−1585.

(2) Ma, M. M.; Bong, D. Controlled Fusion of Synthetic Lipid Membrane Vesicles. *Acc. Chem. Res.* **2013**, *46*, 2988−2997.

(3) Kumar, P.; Guha, S.; Diederichsen, U. SNARE protein analog-mediated membrane fusion. *J. Pept. Sci.* **2015**, *21*, 621−629.

(4) Robson Marsden, H.; Korobko, A. V.; Zheng, T.; Voskuhl, J.; Kros, A. Controlled liposome fusion mediated by SNARE protein mimics. *Biomater. Sci.* **2013**, *1*, 1046.

(5) Robson Marsden, H.; Elbers; Nina, A.; Bomans; Paul, H. H.; Sommerdijk; Nico, A. J. M.; Kros, A. A Reduced SNARE Model for Membrane Fusion. *Angew. Chem., Int. Ed.* **2009**, *48*, 2330−3.

(6) Tomatsu, I.; Marsden, H. R.; Rabe, M.; Versluis, F.; Zheng, T.; Zope, H.; Kros, A. Influence of pegylation on peptide-mediated liposome fusion. *J. Mater. Chem.* **2011**, *21*, 18927−18933.

(7) Versluis, F.; Dominguez, J.; Voskuhl, J.; Kros, A. Coiled-coil driven membrane fusion: zipper-like vs. non-zipper-like peptide orientation. *Faraday Discuss.* **2013**, *166*, 349−359.

(8) Versluis, F.; Voskuhl, J.; van Kolck, B.; Zope, H.; Bremmer, M.; Albregtse, T.; Kros, A. In Situ Modification of Plain Liposomes with Lipidated Coiled Coil Forming Peptides Induces Membrane Fusion. *J. Am. Chem. Soc.* **2013**, *135*, 8057−8062.

(9) Zheng, T. T.; Voskuhl, J.; Versluis, F.; Zope, H. R.; Tomatsu, I.; Marsden, H. R.; Kros, A. Controlling the rate of coiled coil driven membrane fusion. *Chem. Commun.* **2013**, *49*, 3649−3651.

(10) Zope, H. R.; Versluis, F.; Ordas, A.; Voskuhl, J.; Spaink, H. P.; Kros, A. In vitro and in vivo supramolecular modification of biomembranes using a lipidated coiled-coil motif. *Angew. Chem., Int. Ed.* **2013**, *52*, 14247−51.

(11) Voskuhl, J.; Wendeln, C.; Versluis, F.; Fritz, E. C.; Roling, O.; Zope, H.; Schulz, C.; Rinnen, S.; Arlinghaus, H. F.; Ravoo, B. J.; Kros, A. Immobilization of Liposomes and Vesicles on Patterned Surfaces by a Peptide Coiled-Coil Binding Motif. *Angew. Chem., Int. Ed.* **2012**, *51*, 12616−12620.

(12) Meyenberg, K.; Lygina, A. S.; van den Bogaart, G.; Jahn, R.; Diederichsen, U. SNARE derived peptide mimic inducing membrane fusion. *Chem. Commun.* **2011**, *47*, 9405−9407.

(13) Pähler, G.; Lorenz, B.; Janshoff, A. Impact of peptide clustering on unbinding forces in the context of fusion mimetics. *Biochem. Biophys. Res. Commun.* **2013**, *430*, 938−943.

(14) Pähler, G.; Panse, C.; Diederichsen, U.; Janshoff, A. Coiled-Coil Formation on Lipid Bilayers-Implications for Docking and Fusion Efficiency. *Biophys. J.* **2012**, *103*, 2295−2303.

(15) Rabe, M.; Schwieger, C.; Zope, H. R.; Versluis, F.; Kros, A. Membrane Interactions of Fusogenic Coiled-Coil Peptides: Implications for Lipopeptide Mediated Vesicle Fusion. *Langmuir* **2014**, *30*, 7724−35.

(16) Grigoryan, G.; Keating, A. E. Structural specificity in coiled-coil interactions. *Curr. Opin. Struct. Biol.* **2008**, *18*, 477−483.

(17) Litowski, J. R.; Hodges, R. S. Designing heterodimeric two-stranded alpha-helical coiled-coils. Effects of hydrophobicity and alpha-helical propensity on protein folding, stability, and specificity. *J. Biol. Chem.* **2002**, *277*, 37272−9.

(18) Pluhackova, K.; Wassenaar, T. A.; Kirsch, S.; Böckmann, R. A. Spontaneous Adsorption of Coiled-Coil Model Peptides K and E to a Mixed Lipid Bilayer. *J. Phys. Chem. B* **2015**, *119*, 4396−4408.

(19) Bulacu, M.; Sevink, G. J. A. Computational insight in the role of fusogenic lipopeptides at the onset of liposome fusion. *Biochim. Biophys. Acta, Biomembr.* **2015**, *1848*, 1716−1725.

(20) Chernomordik, L. V.; Kozlov, M. M. Protein-lipid interplay in fusion and fission of biological membranes. *Annu. Rev. Biochem.* **2003**, *72*, 175−207.

(21) Rabe, M.; Boyle, A.; Zope, H.; Versluis, F.; Kros, A. Determination of oligomeric states of peptide complexes using thermal unfolding curves. *Biopolymers* **2015**, *104*, 65−72.

(22) Chen, Y.-H.; Yang, J. T.; Chau, K. H. Determination of the helix and *β* form of proteins in aqueous solution by circular dichroism. *Biochemistry* **1974**, *13*, 3350−3359.

(23) Gans, P. J.; Lyu, P. C.; Manning, M. C.; Woody, R. W.; Kallenbach, N. R. The helix−coil transition in heterogeneous peptides with specific side-chain interactions: Theory and comparison with CD spectral data. *Biopolymers* **1991**, *31*, 1605−1614.

(24) Cooper, T. M.; Woody, R. W. The Effect of Conformation on the Cd of Interacting Helices - a Theoretical-Study of Tropomyosin. *Biopolymers* **1990**, *30*, 657−676.

(25) Barth, A. Infrared spectroscopy of proteins. *Biochim. Biophys. Acta, Bioenerg.* **2007**, *1767*, 1073−1101.

(26) Heimburg, T.; Schuenemann, J.; Weber, K.; Geisler, N. Specific Recognition of Coiled Coils by Infrared Spectroscopy: Analysis of the Three Structural Domains of Type III Intermediate Filament Proteins. *Biochemistry* **1996**, *35*, 1375−1382.

(27) Reisdorf, W. C., Jr.; Krimm, S. Infrared amide I′ band of the coiled coil. *Biochemistry* **1996**, *35*, 1383−6.

(28) Heimburg, T.; Schünemann, J.; Weber, K.; Geisler, N. FTIR-Spectroscopy of Multistranded Coiled Coil Proteins. *Biochemistry* **1999**, *38*, 12727−12734.

(29) Manas, E. S.; Getahun, Z.; Wright, W. W.; DeGrado, W. F.; Vanderkooi, J. M. Infrared Spectra of Amide Groups in a-Helical Proteins: Evidence for Hydrogen Bonding between Helices and Water. *J. Am. Chem. Soc.* **2000**, *122*, 9883−9890.

(30) Walsh, S. T.; Cheng, R. P.; Wright, W. W.; Alonso, D. O.; Daggett, V.; Vanderkooi, J. M.; DeGrado, W. F. The hydration of amides in helices; a comprehensive picture from molecular dynamics, IR, and NMR. *Protein Sci.* **2003**, *12*, 520−31.

(31) Bi, X.; Flach, C. R.; Pérez-Gil, J.; Plasencia, I.; Andreu, D.; Oliveira, E.; Mendelsohn, R. Secondary Structure and Lipid Interactions of the N-Terminal Segment of Pulmonary Surfactant SP-C in Langmuir Films: IR Reflection−Absorption Spectroscopy and Surface Pressure Studies†. *Biochemistry* **2002**, *41*, 8385−8395.

(32) Lewis, R. N. A. H.; Prenner, E. J.; Kondejewski, L. H.; Flach, C. R.; Mendelsohn, R.; Hodges, R. S.; McElhaney, R. N. Fourier Transform Infrared Spectroscopic Studies of the Interaction of the Antimicrobial Peptide Gramicidin S with Lipid Micelles and with Lipid Monolayer and Bilayer Membranes. *Biochemistry* **1999**, *38*, 15193−15203.

(33) Mukherjee, S.; Chowdhury, P.; Gai, F. Infrared Study of the Effect of Hydration on the Amide I Band and Aggregation Properties of Helical Peptides. *J. Phys. Chem. B* **2007**, *111*, 4596−4602.

(34) Mukherjee, S.; Chowdhury, P.; DeGrado, W. F.; Gai, F. Site-specific hydration status of an amphipathic peptide in AOT reverse micelles. *Langmuir* **2007**, *23*, 11174−11179.

(35) Tadesse, L.; Nazarbaghi, R.; Walters, L. Isotopically enhanced infrared spectroscopy: a novel method for examining secondary structure at specific sites in conformationally heterogeneous peptides. *J. Am. Chem. Soc.* **1991**, *113*, 7036−7037.

(36) Decatur, S. M.; Antonic, J. Isotope-Edited Infrared Spectroscopy of Helical Peptides. *J. Am. Chem. Soc.* **1999**, *121*, 11914−11915.

(37) Barber-Armstrong, W.; Donaldson, T.; Wijesooriya, H.; Silva, R. A. G. D.; Decatur, S. M. Empirical Relationships between Isotope-Edited IR Spectra and Helix Geometry in Model Peptides. *J. Am. Chem. Soc.* **2004**, *126*, 2339−2345.

(38) Starzyk, A.; Barber-Armstrong, W.; Sridharan, M.; Decatur, S. M. Spectroscopic evidence for backbone desolvation of helical peptides by 2,2,2-trifluoroethanol: an isotope-edited FTIR study. *Biochemistry* **2005**, *44*, 369−76.

(39) Decatur, S. M. Elucidation of Residue-Level Structure and Dynamics of Polypeptides via Isotope-Edited Infrared Spectroscopy. *Acc. Chem. Res.* **2006**, *39*, 169−175.

(40) Kubelka, G. S.; Kubelka, J. Site-Specific Thermodynamic Stability and Unfolding of a de Novo Designed Protein Structural Motif Mapped by 13C Isotopically Edited IR Spectroscopy. *J. Am. Chem. Soc.* **2014**, *136*, 6037−6048.

(41) Fesinmeyer, R. M.; Peterson, E. S.; Dyer, R. B.; Andersen, N. H. Studies of helix fraying and solvation using 13C′ isotopomers. *Protein Sci.* **2005**, *14*, 2324−2332.

(42) Hendler, R. W.; Shrager, R. I. Deconvolutions based on singular value decomposition and the pseudoinverse: a guide for beginners. *J. Biochem. Biophys. Methods* **1994**, *28*, 1−33.

(43) Henry, E. R.; Hofrichter, J. [8] Singular value decomposition: Application to analysis of experimental data. In *Methods in Enzymology*, Ludwig Brand, M. L. J., Ed.; Academic Press, 1992; Vol. Vol. *210*, pp 129−192.

(44) Brewer, S. H.; Tang, Y.; Vu, D. M.; Gnanakaran, S.; Raleigh, D. P.; Dyer, R. B. Temperature dependence of water interactions with the amide carbonyls of alpha-helices. *Biochemistry* **2012**, *51*, 5293−9.

(45) Breslauer, K. J. [10] Extracting thermodynamic data from equilibrium melting curves for oligonucleotide order-disorder transitions. In *Methods in Enzymology*; Michael, L. Johnson, G. K. A., Ed.; Academic Press: New York, 1995; Vol. *259*, pp 221−242.

(46) Doyle, C. M.; Rumfeldt, J. A.; Broom, H. R.; Broom, A.; Stathopulos, P. B.; Vassall, K. A.; Almey, J. J.; Meiering, E. M. Energetics of oligomeric protein folding and association. *Arch. Biochem. Biophys.* **2013**, *531*, 44−64.

(47) Greenfield, N. J. Using circular dichroism collected as a function of temperature to determine the thermodynamics of protein unfolding and binding interactions. *Nat. Protoc.* **2006**, *1*, 2527−35.

(48) Dragan, A. I.; Privalov, P. L. Unfolding of a Leucine zipper is not a Simple Two-state Transition. *J. Mol. Biol.* **2002**, *321*, 891−908.

(49) Segrest, J. P.; De Loof, H.; Dohlman, J. G.; Brouillette, C. G.; Anantharamaiah, G. M. Amphipathic helix motif: Classes and properties. *Proteins: Struct., Funct., Genet.* **1990**, *8*, 103−117.

(50) Mishra, V. K.; Palgunachari, M. N.; Segrest, J. P.; Anantharamaiah, G. M. Interactions of synthetic peptide analogs of the class A amphipathic helix with lipids. Evidence for the snorkel hypothesis. *J. Biol. Chem.* **1994**, *269*, 7185−91.

(51) Segrest, J. P.; Jones, M. K.; Mishra, V. K.; Anantharamaiah, G. M. Experimental and computational studies of the interactions of amphipathic peptides with lipid surfaces. In *Current Topics in Membranes*; Sidney, A., Simon, T. J. M., Eds.; Academic Press: New York, 2002; Vol. *52*, pp 397−435.

(52) Kubelka, J. Multivariate Analysis of Spectral Data with Frequency Shifts: Application to Temperature Dependent Infrared Spectra of Peptides and Proteins. *Anal. Chem.* **2013**, *85*, 9588−9595.

(53) Andrushchenko, V. V.; Vogel, H. J.; Prenner, E. J. Optimization of the hydrochloric acid concentration used for trifluoroacetate removal from synthetic peptides. *J. Pept. Sci.* **2007**, *13*, 37−43.

(54) Barth, A.; Zscherp, C. What vibrations tell about proteins. *Q. Rev. Biophys.* **2002**, *35*, 369−430.

(55) Paschek, D.; Puhse, M.; Perez-Goicochea, A.; Gnanakaran, S.; Garcia, A. E.; Winter, R.; Geiger, A. The Solvent-Dependent Shift of the Amide I Band of a Fully Solvated Peptide as a Local Probe for the Solvent Composition in the Peptide/Solvent Interface. *ChemPhysChem* **2008**, *9*, 2742−2750.

(56) Kučerka, N.; Gallová, J.; Uhríková, D.; Balgavý, P.; Bulacu, M.; Marrink, S.-J.; Katsaras, J. Areas of Monounsaturated Diacylphosphatidylcholines. *Biophys. J.* **2009**, *97*, 1926−1932.

(57) Wang, T.; Lau, W. L.; DeGrado, W. F.; Gai, F. T-Jump Infrared Study of the Folding Mechanism of Coiled-Coil GCN4-p1. *Biophys. J.* **2005**, *89*, 4180−4187.

(58) Imamura, H.; Isogai, Y.; Takekiyo, T.; Kato, M. Effect of pressure on the secondary structure of coiled coil peptide GCN4-p1. *Biochim. Biophys. Acta, Proteins Proteomics* **2010**, *1804*, 193−198.

(59) Glasoe, P. K.; Long, F. A. Use of glass electrodes to measure acidities in deuterium oxide. *J. Phys. Chem.* **1960**, *64*, 188−190.

(60) Meier, R. J. On art and science in curve-fitting vibrational spectra. *Vib. Spectrosc.* **2005**, *39*, 266−269.